Supporting Information
for

Tetracoordinate silicon complexes of 1,2-bis(indol-2-yl)benzene as blue-emitting dyes in the solid state

Takayuki Tanaka* and Atsuhiro Osuka*

Department of Chemistry, Graduate School of Science, Kyoto University, Sakyo-ku, Kyoto 606-8502 (Japan)

E-mail: taka@kuchem.kyoto-u.ac.jp; osuka@ kuchem.kyoto-u.ac.jp

Contents

1. Instrumentation and Materials

Commercially available solvents and reagents were used without further purification unless otherwise noted. The spectroscopic grade solvents were used as solvents for all spectroscopic studies. Silica gel column chromatography was performed on Wakogel C-300. Alumina column chromatography was performed on Sumitomo γ-Alumina. Thin-layer chromatography (TLC) was carried out on aluminum sheets coated with silica gel 60 F254 (Merck 5554). UV/Visible absorption spectra were recorded on Shimadzu UV-3600 spectrometers. Fluorescence spectra were recorded on a Shimadzu RF-5300PC spectrometer. Absolute fluorescence quantum yields were determined on a HAMAMATSU C9920-02S. ^{1}H, ^{13}C and ^{29}Si NMR spectra were recorded on a JEOL ECA-600 spectrometer (operating as 600 MHz for ^{1}H, 151 MHz for ^{13}C, and 119 MHz for ^{29}Si) using the residual solvents as the internal references for ^{1}H (δ = 7.26 ppm in $CDCl_3$ and δ = 2.08 ppm in toluene-d_8) and for ^{13}C (δ = 77.16 ppm in $CDCl_3$) and tetramethylsilane as the external reference for ^{29}Si (δ = 0.00 ppm in toluene-d_8). High-resolution atmospheric-pressure-chemical-ionization time-of-flight mass-spectroscopy (HR-APCI-TOF-MS) was recorded on a BRUKER micrOTOF model using positive mode. Mass spectra were recorded on a Shimadzu AXIMA-CFRplus using positive-MALDI-TOF method with matrix. Single-crystal diffraction analysis data were collected at –180 °C with a Rigaku XtaLAB P200 by using graphite monochromated Cu-$K\alpha$ radiation (λ = 1.54187 Å). The structures were solved by direct methods (SHELXS-97) and refined with full-matrix least square technique (SHELXL-97).

2. Experimental Section

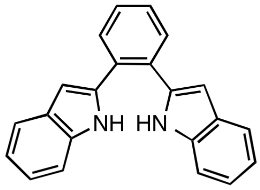

1,2-Bis(indol-2-yl)benzene (1).

To a dry Schlenk tube, indole-2-boronic acid pinacolate ester (1.40 g, 5.74 mmol), [1,1′-bis(diphenylphosphino)ferrocene]dichloropalladium(II) (141 mg, 7.5 mol%), and dry dioxane (5.0 mL) were added. Degassed K_2CO_3 aq. (1.0 mL, 4.59 mmol) and 1,2-diiodobenzene (0.30 mL, 2.30 mmol) were then added, and the mixture was deoxygenated through freeze–pump–thaw cycle. The mixture was stirred at 90 °C for 24 h. After cooling to room temperature, the reaction was quenched by addition of water, extracted with ethyl acetate and washed by brine. The organic phase was dried over anhydrous Na_2SO_4. The solvent was removed under reduced pressure and the residue was purified by column chromatography on silica with dichloromethane as an eluent. Recrystallization from dichloromethane/*n*-hexane afforded 1,2-bis(indol-2-yl)benzene (**1**) as a white solid (492 mg, 1.59 mmol, 70%).

1; ^{1}H NMR ($CDCl_3$) δ (ppm): 7.96 (s, 2H, NH), 7.68 (dd, J = 3.2, 5.5 Hz, 2H, benzene-H), 7.62 (m, 2H, indole-H), 7.45 (dd, J = 3.2, 5.5 Hz, 2H, benzene-H), 7.14-7.09 (m, 6H, indole-H) and 6.71 (d, 2H, J = 2.3 Hz, indole-H); ^{13}C NMR ($CDCl_3$) δ (ppm): 137.16, 136.67, 130.95, 130.90, 128.57, 128.47, 122.57, 120.72, 120.32, 111.24, and 102.78; HR-APCI-TOF-MS m/z = 309.1375, calcd. for $C_{22}H_{16}N_2$ = 309.1386 $[M+H]^+$. UV-vis (CH_2Cl_2) λ_{max} ([$M^{-1}cm^{-1}$]) = 293 (23000) nm; Fluorescence (CH_2Cl_2, λ_{ex} = 340 nm) λ_{max} = 422 nm, ϕ_F = 0.58; Fluorescence (powder, λ_{ex} = 330 nm) λ_{max} = 440 and 471 nm, ϕ_F = 0.09.

General procedure for the synthesis of silicon complexes

Potassium bis(trimethylsilyl)amide (0.5 M in toluene, 2.4 equiv.) was added to a solution of **1** in THF at 0 °C. After 15 min, dialkyl/diaryldichlorosilane (1.2 equiv.) was added dropwise, and the solution was allowed to gradually warm to room temperature over 12 h, at which time the reaction was quenched with a mixture of water and ethyl acetate. The organic extracts were washed with water and brine, dried over anhydrous Na_2SO_4, and evaporated under reduced pressure. The residue was purified by column chromatography on silica with a mixture of dichloromethane and *n*-hexane as eluent to yield silicon complexes as off-white solids.

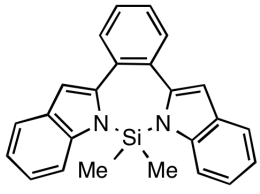

According to the general procedure, dimethyldichlorosilane (0.046 mL, 0.39 mmol) was reacted with **1** (100 mg, 0.32 mmol). Yield; 69 mg (0.19 mmol, 58%).

2a; ^{1}H NMR (toluene-d_8, –80 °C) δ (ppm): 7.70 (d, J = 7.8 Hz, 2H, indole-H), 7.45 (dd, J = 5.5, 3.7 Hz, 2H, phenyl-H), 7.37 (J = 8.7 Hz, 2H, indole-H), 7.33 (t, J = 7.3 Hz, 2H, indole-H), 7.25 (t, J = 7.3 Hz, 2H, indole-H), 7.10 (dd, J = 5.5, 3.7 Hz, 2H, phenyl-H), 6.57 (s, 2H, indole-H), 0.68 (s, 3H, Me), and –0.18 (s, 3H, Me); ^{13}C NMR ($CDCl_3$, 60 °C) δ (ppm): 144.19, 141.39, 133.31, 131.69, 131.48, 128.90, 122.51, 120.97, 120.90, 112.89, 108.47 and 2.87; ^{29}Si{^{1}H} (toluene-d_8, –80 °C) 1.51 ppm; HR-APCI-TOF-MS m/z =365.1488, calcd. for $C_{24}H_{20}N_2Si_1$ = 365.1469 $[M+H]^+$; UV-vis (CH_2Cl_2) λ_{max} ([$M^{-1}cm^{-1}$]) = 293 (26000) nm; Fluorescence (CH_2Cl_2, λ_{ex} = 330 nm) λ_{max} = 395 nm, ϕ_F = 0.58; Fluorescence (powder, λ_{ex} = 330 nm) λ_{max} = 379 nm, ϕ_F = 0.55.

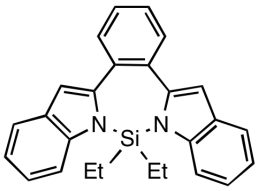

According to the general procedure, diethyldichlorosilane (0.12 mL, 0.78 mmol) was reacted with **1** (200 mg, 0.65 mmol). Yield; 103 mg (0.26 mmol, 40%).

2b; ^{1}H NMR (toluene-d_8, –80 °C) δ (ppm): 7.70 (d, J = 7.8 Hz, 2H, indole-H), 7.48 (dd, J = 5.5, 3.7 Hz, 2H, phenyl-H), 7.35 (J = 8.7 Hz, 2H, indole-H), 7.32 (t, J = 7.6 Hz, 2H, indole-H), 7.27 (t, J = 7.6 Hz, 2H, indole-H), 7.11 (dd, J = 5.5, 3.7 Hz, 2H, phenyl-H), 6.55 (s, 2H, indole-H), 1.34 (br, 2H, Et), 0.87 (t, J = 7.3 Hz, 3H, Et), 0.52 (br, 2H, Et) and 0.45 (t, J = 7.3 Hz, 3H, Et); ^{13}C NMR ($CDCl_3$, 60 °C) δ (ppm): 144.25, 141.42, 133.56, 131.49, 131.33, 128.85, 122.56, 120.91, 120.84, 112.98, 108.57, 6.80 and 6.76; ^{29}Si{^{1}H} (toluene-d_8, –80 °C) 3.03 ppm; HR-APCI-TOF-MS m/z =393.1783, calcd. for $C_{26}H_{24}N_2Si_1$ = 393.1782 $[M+H]^+$; UV-vis (CH_2Cl_2) λ_{max} ([$M^{-1}cm^{-1}$]) = 294 (27000) nm; Fluorescence (CH_2Cl_2, λ_{ex} = 330 nm) λ_{max} = 394 nm, ϕ_F = 0.58; Fluorescence (powder, λ_{ex} = 330 nm) λ_{max} = 390 nm, ϕ_F = 0.49.

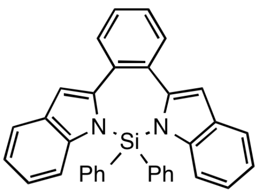

According to the general procedure, diphenyldichlorosilane (0.30 mL, 1.17 mmol) was reacted with **1** (300 mg, 0.97 mmol). Yield; 461 mg (0.94 mmol, 97%).

2c; ^{1}H NMR ($CDCl_3$, 50 °C) δ (ppm): 7.60 (d, J = 7.8 Hz, 2H, indole-H), 7.53 (d, J = 6.9 Hz, 4H, Si-Ph), 7.51 (d, J = 7.8 Hz, 2H, Si-Ph), 7.40 (dd, J = 5.5, 3.7 Hz, 2H, phenyl-H), 7.34 (t, J = 7.8 Hz, 4H, Si-Ph), 7.19 (dd, J = 5.5, 3.7 Hz, 2H, phenyl-H), 7.06 (t, J = 7.8 Hz, 2H, indole-H), 6.88 (s, 2H, indole-H), 6.78 (t, J = 7.4 Hz, 2H, indole-H), and 6.43 (d, J = 7.8 Hz, 2H, indole-H); ^{13}C NMR ($CDCl_3$) δ (ppm): 145.20, 142.88, 136.91, 132.41, 132.32, 132.03, 131.99, 129.79, 128.47, 128.35, 121.45, 120.96, 120.33, 115.36, and 109.30; ^{29}Si{^{1}H} (toluene-d_8, –80 °C) –22.09 ppm; HR-APCI-TOF-MS m/z =489.1785, calcd. for $C_{34}H_{24}N_2Si_1$ = 489.1782 $[M+H]^+$; UV-vis (CH_2Cl_2) λ_{max} ([$M^{-1}cm^{-1}$]) = 294 (25000) nm; Fluorescence (CH_2Cl_2, λ_{ex} = 350 nm) λ_{max} = 421 nm, ϕ_F = 0.65;

Fluorescence (powder, λ_{ex} = 330 nm) λ_{max} = 388 nm, ϕ_F = 0.54.

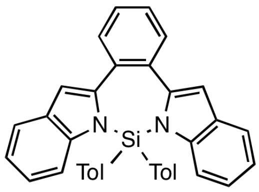

According to the general procedure, di(*p*-tolyl)dichlorosilane (0.15 mL, 0.58 mmol) was reacted with **1** (150 mg, 0.49 mmol). Yield; 155 mg (0.30 mmol, 62%).

2d; ^{1}H NMR (CD_2Cl_2, r.t.) δ (ppm): 7.56 (d, *J* = 7.8 Hz, 2H, indole-H), 7.40 (dd, *J* = 5.7, 3.5 Hz, 2H, phenyl-H), 7.34 (d, *J* = 7.8 Hz, 4H, tolyl-H), 7.21 (dd, *J* = 5.7, 3.5 Hz, 2H, phenyl-H), 7.15 (d, *J* = 7.8 Hz, 4H, tolyl-H), 7.01 (t, *J* = 7.3 Hz, 2H, indole-H), 6.86 (s, 2H), 6.74 (t, *J* = 7.3 Hz, 2H, indole-H), 6.42 (d, *J* = 8.7 Hz, 2H, indole-H) and 2.36 (s, 6H, tolyl-Me); ^{13}C NMR ($CDCl_3$) δ (ppm): 145.27, 142.92, 142.21, 136.92, 132.47, 132.25, 131.93, 129.13, 128.39, 126.34, 121.33, 120.82, 120.23, 115.48, 109.14, and 21.95; ^{29}Si{^{1}H} (toluene-d_8, –80 °C) –22.21 ppm; HR-APCI-TOF-MS *m/z* =517.2105, calcd. for $C_{36}H_{28}N_2Si_1$ = 517.2095 [*M*+H]$^+$; UV-vis (CH_2Cl_2) λ_{max} ([$M^{-1}cm^{-1}$]) = 295 (26000) nm; Fluorescence (CH_2Cl_2, λ_{ex} = 340 nm) λ_{max} = 419 nm, ϕ_F = 0.62; Fluorescence (powder, λ_{ex} = 330 nm) λ_{max} = 386 nm, ϕ_F = 0.71.

3. NMR Spectra

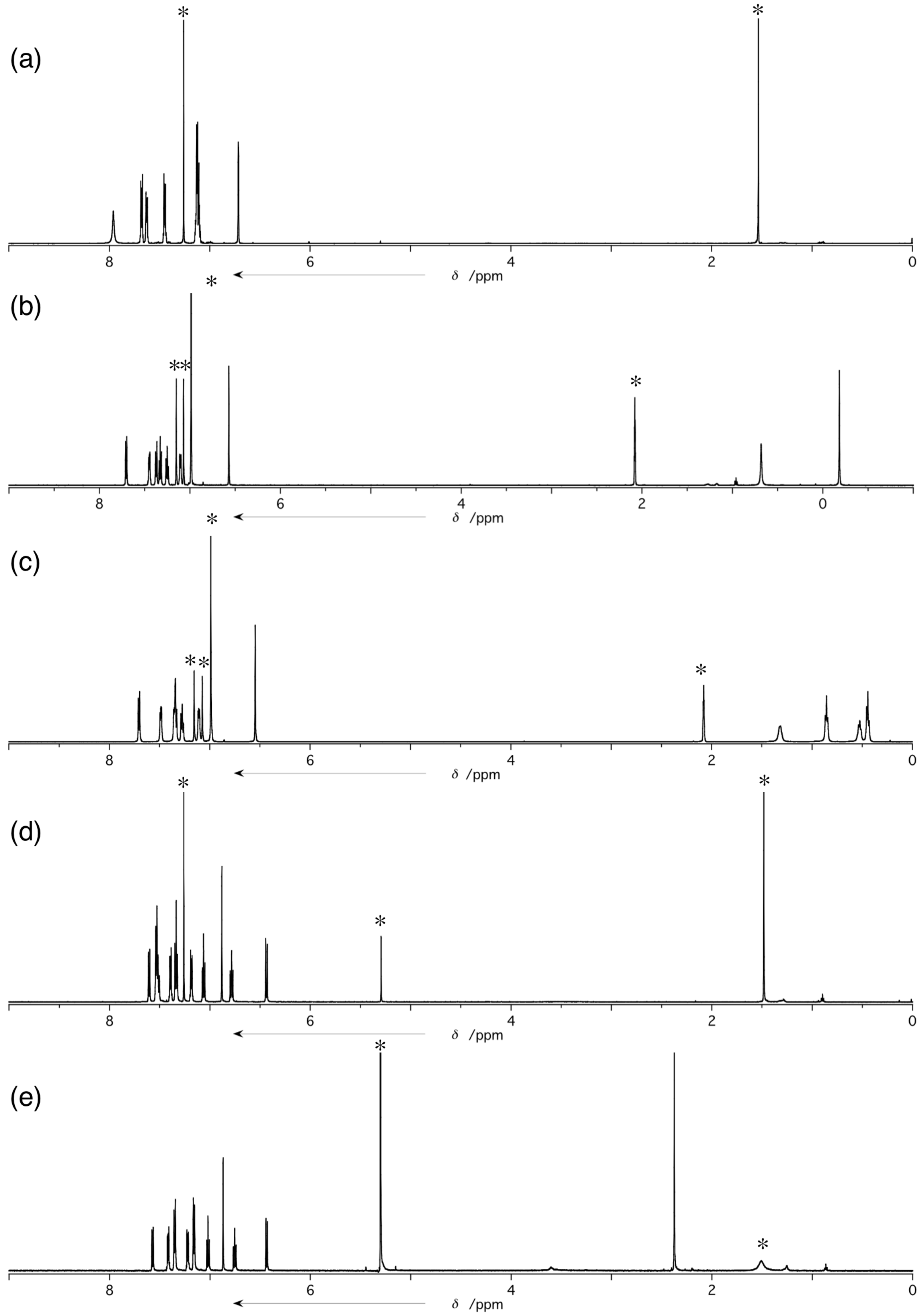

Figure S1. ^{1}H NMR spectra of (a) **1** at r.t. in $CDCl_3$, (b) **2a** at –80 ºC in toluene-d_8, (b) **2b** –80 ºC in toluene-d_8, (d) **2c** at 50 ºC in $CDCl_3$, and (e) **2d** at r.t. in CD_2Cl_2. * means residual solvent peaks.

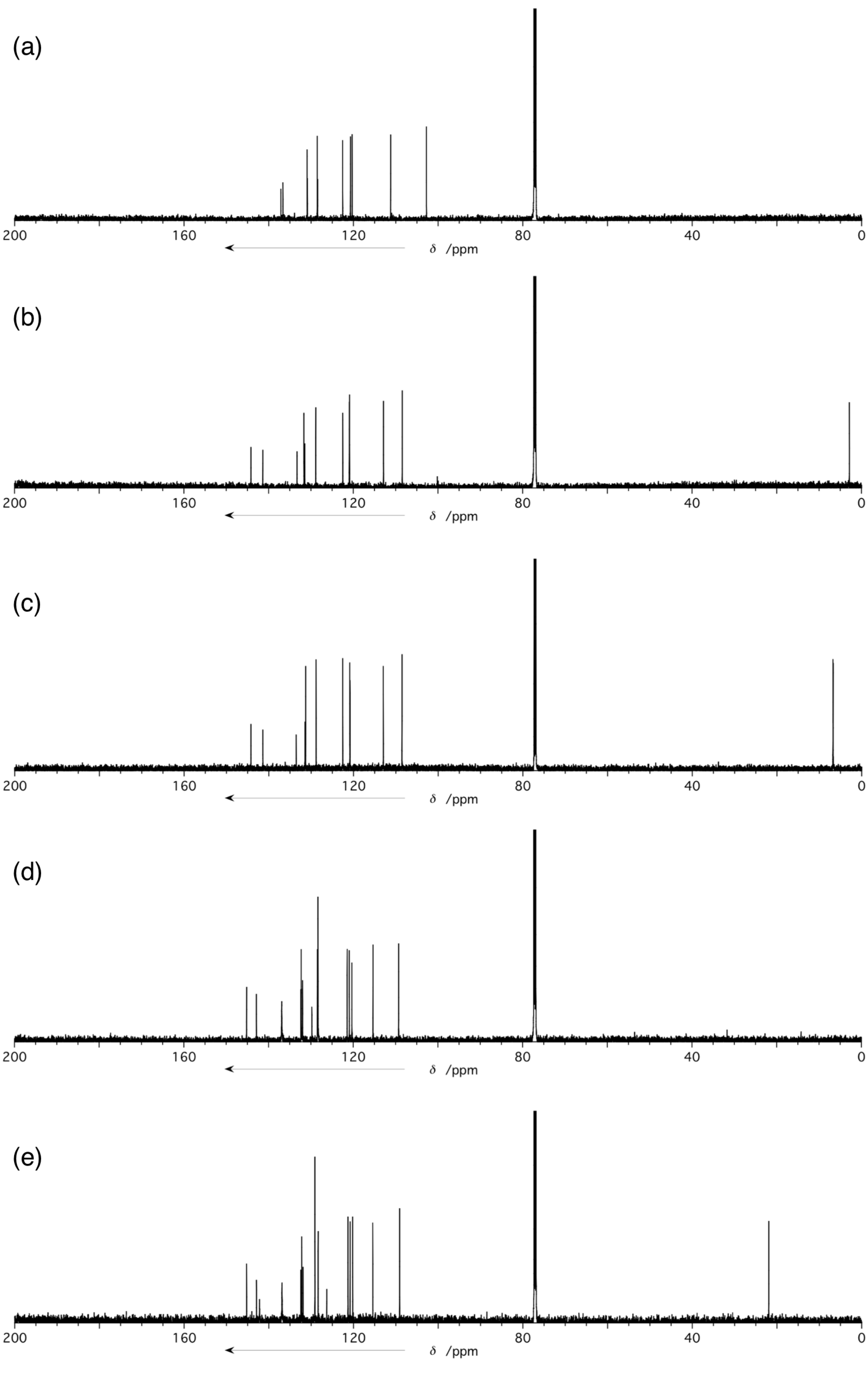

Figure S2. ^{13}C NMR spectra of (a) **1** at r.t., (b) **2a** at 60 ºC, (b) **2b** at 60 ºC, (d) **2c** at r.t., and (c) **2d** at r.t. in $CDCl_3$.

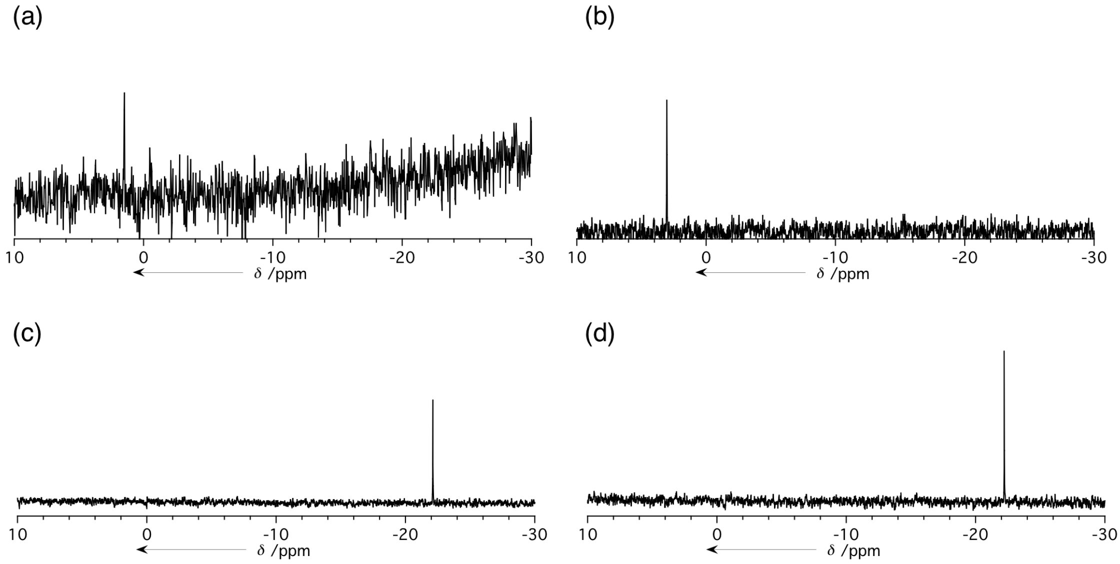

Figure S3. $^{29}Si\{^{1}H\}$ NMR spectra of (a) **2a**, (b) **2b**, (c) **2c**, and (d) **2d** at –80 °C in toluene-d_8.

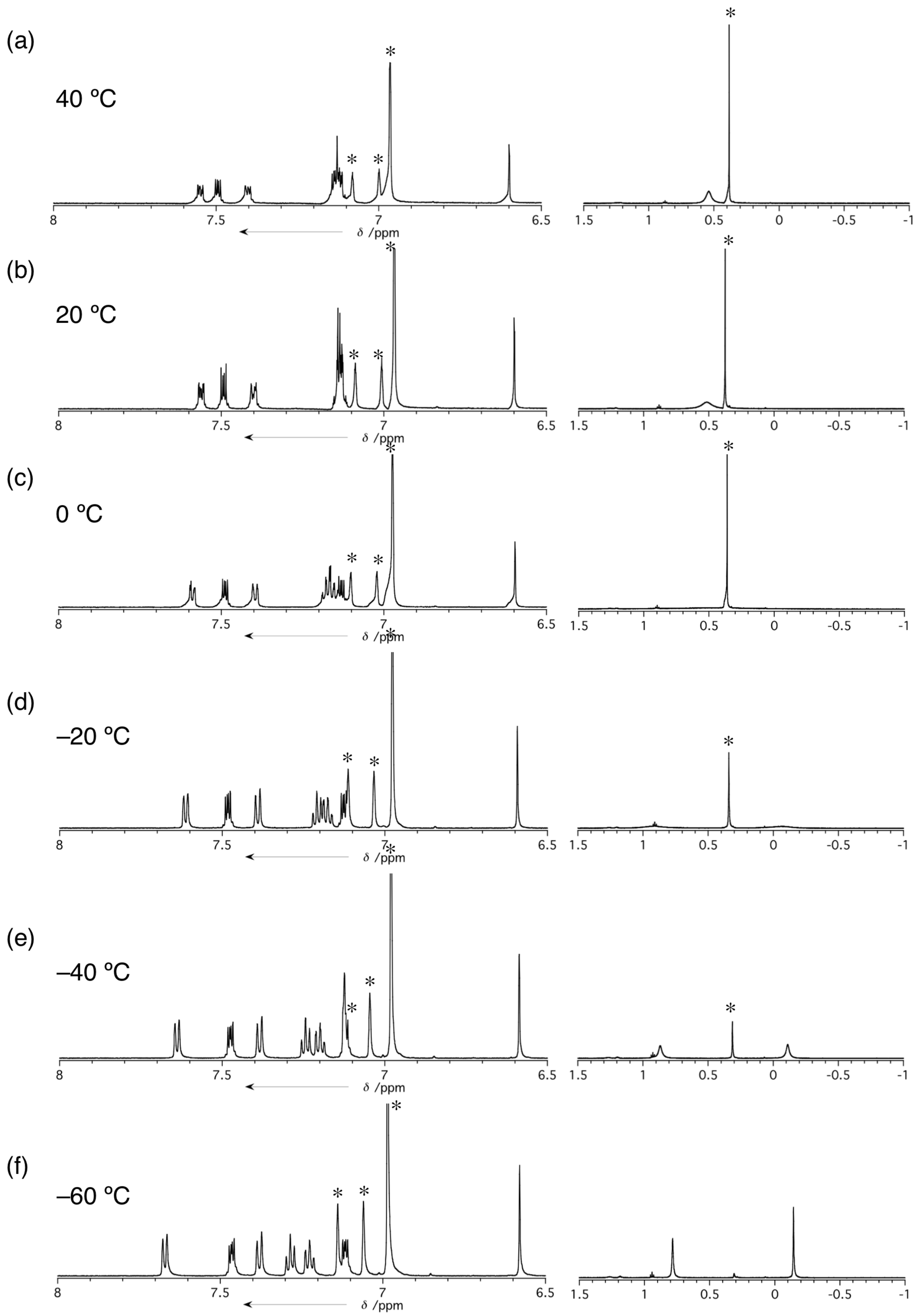

Figure S4. Variable-temperature ^{1}H NMR spectra of **2a** in toluene-d_8. * means residual solvent peaks.

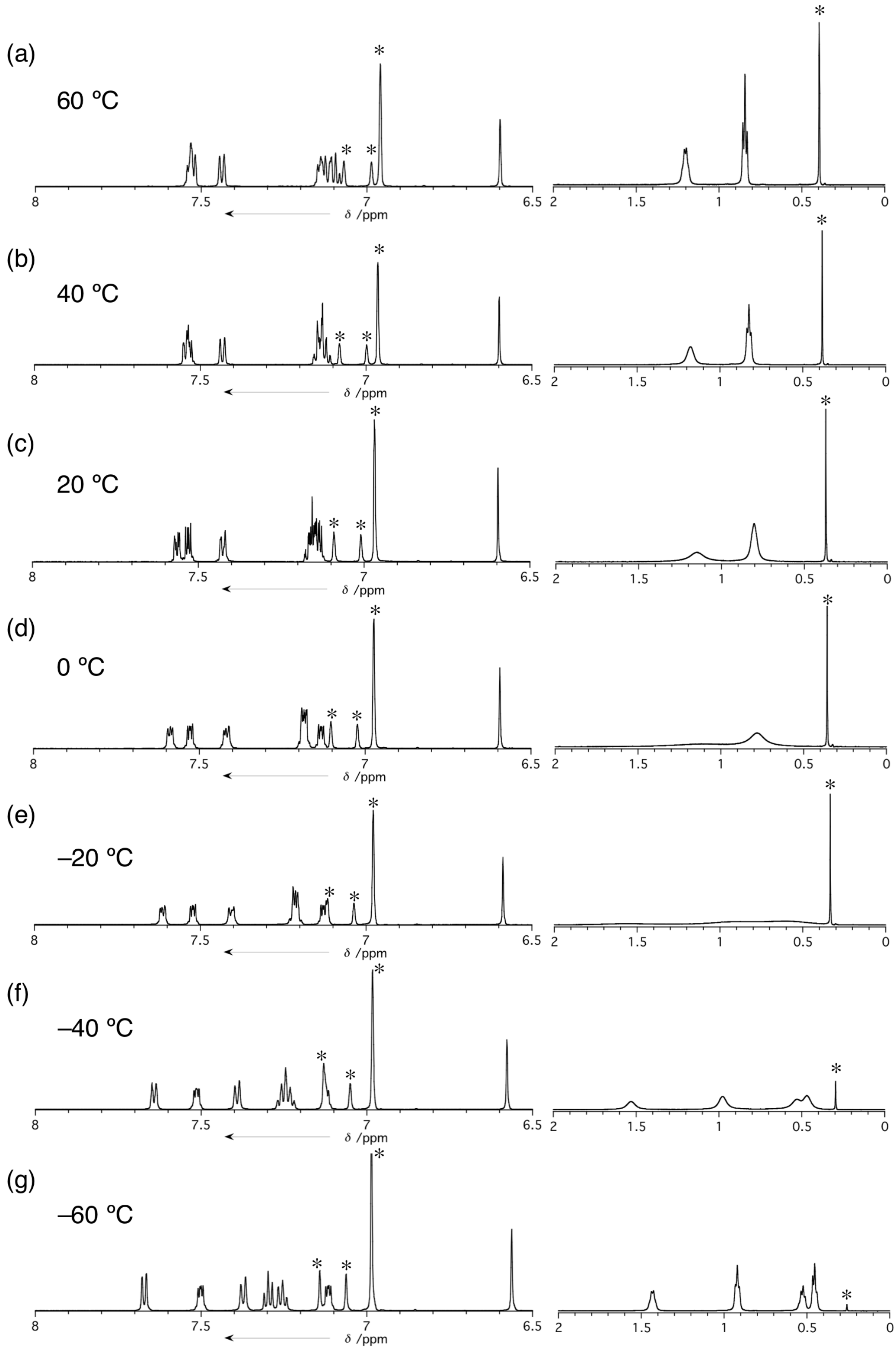

Figure S5. Variable-temperature ^{1}H NMR spectra of **2b** in toluene-d_8. * means residual solvent peaks.

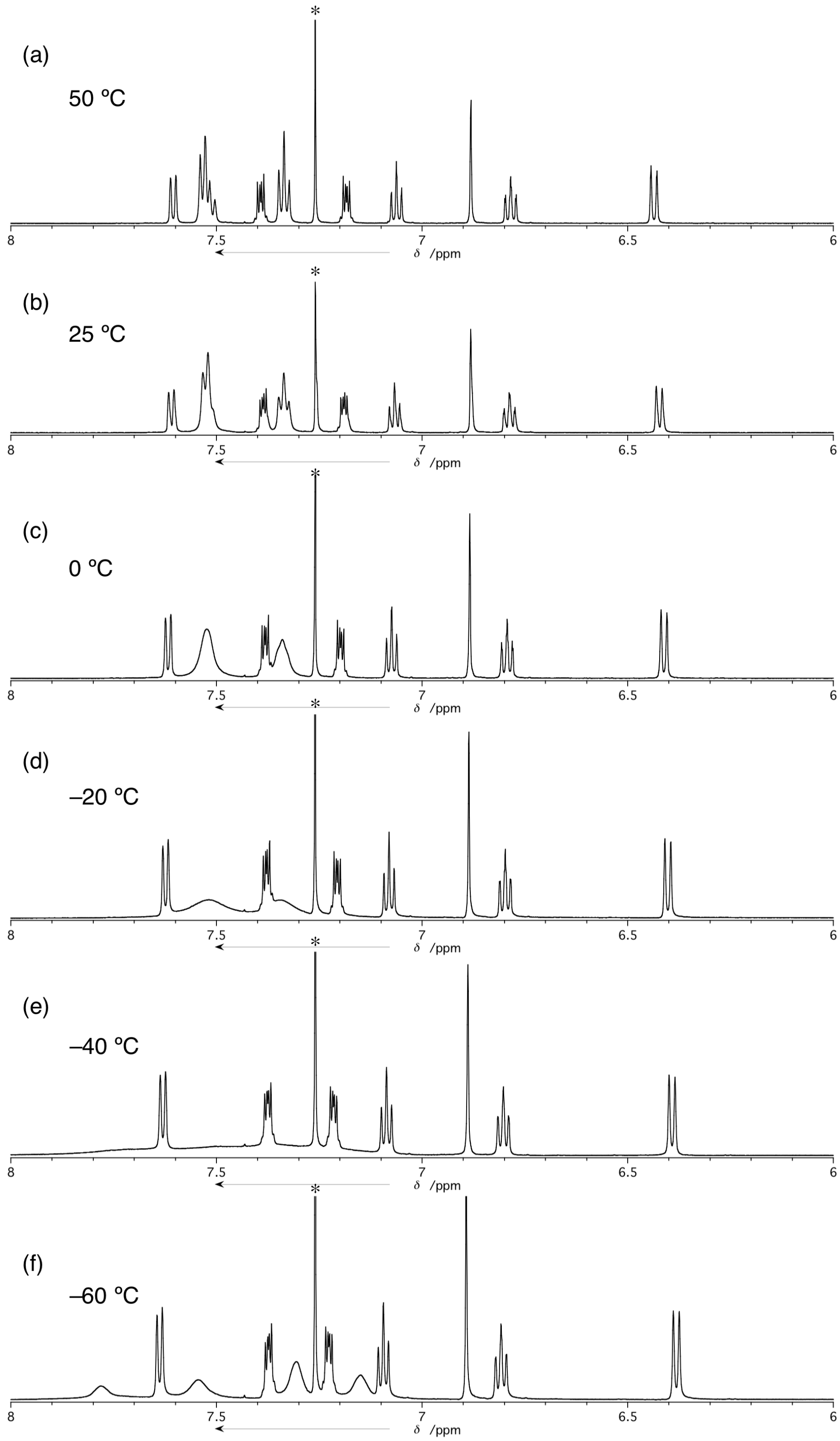

Figure S6. Variable-temperature ^{1}H NMR spectra of **2c** in $CDCl_3$. * means residual solvent peaks.

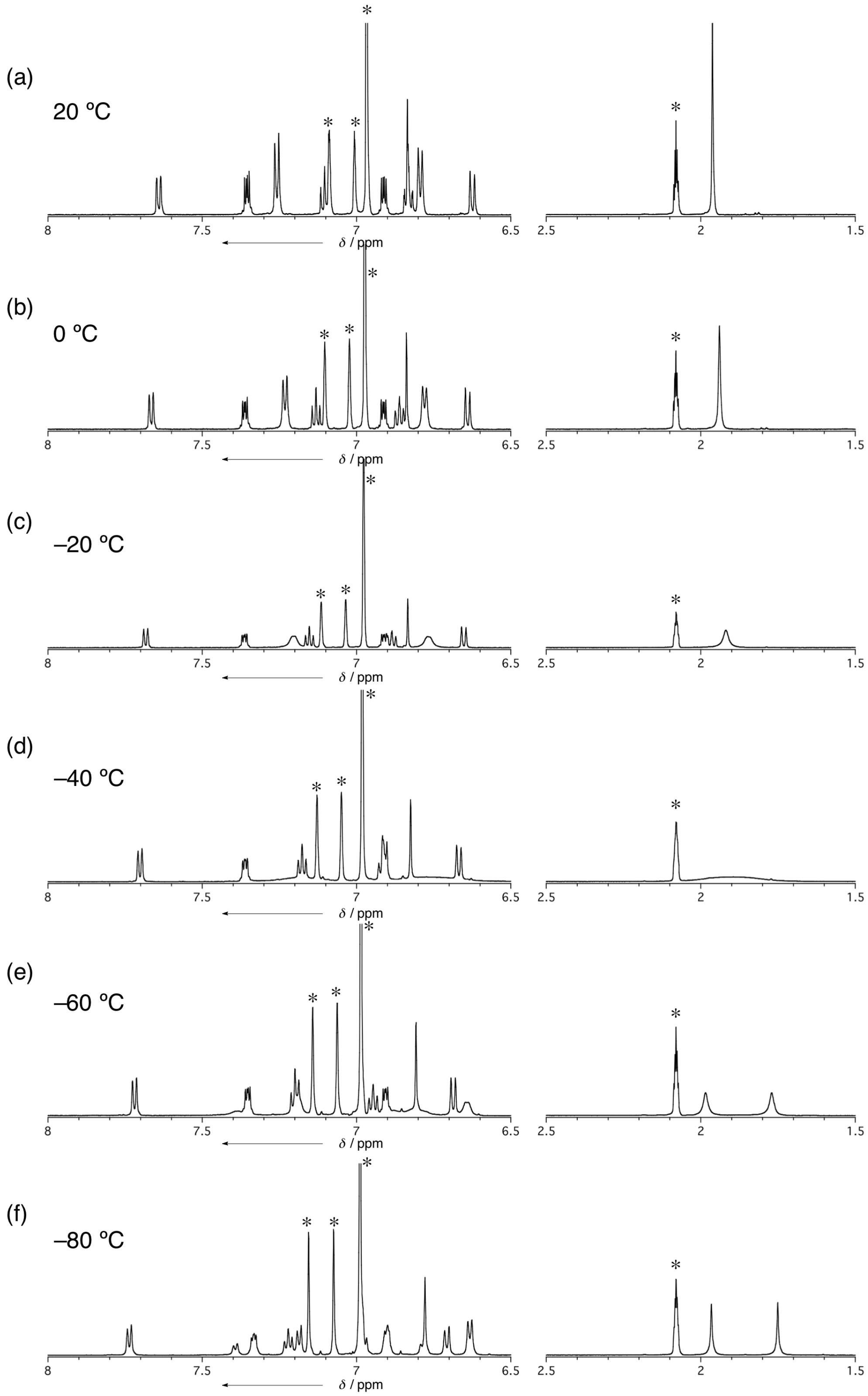

Figure S7. Variable-temperature ^{1}H NMR spectra of **2d** in toluene-d_8. * means residual solvent peaks.

Table S1. Simulated exchange rate constants (k) for **2a** and **2d** at various temperatures.[a]

(a) **2a** in toluene-d_8 | (b) **2d** in toluene-d_8

T [K]	k [s^{-1}]	T (K)	k [s^{-1}]
313	18000	273	40000
293	8200	253	3000
273	1200	233	290
253	350	213	20
233	44	203	4.0

[a] The rate constants (k) were determined by simulations of singlet peaks observed at 0.54 ppm at 313 K for **2a**, and at 2.36 ppm at 273 K for **2d** by the DNMR program.[S1]

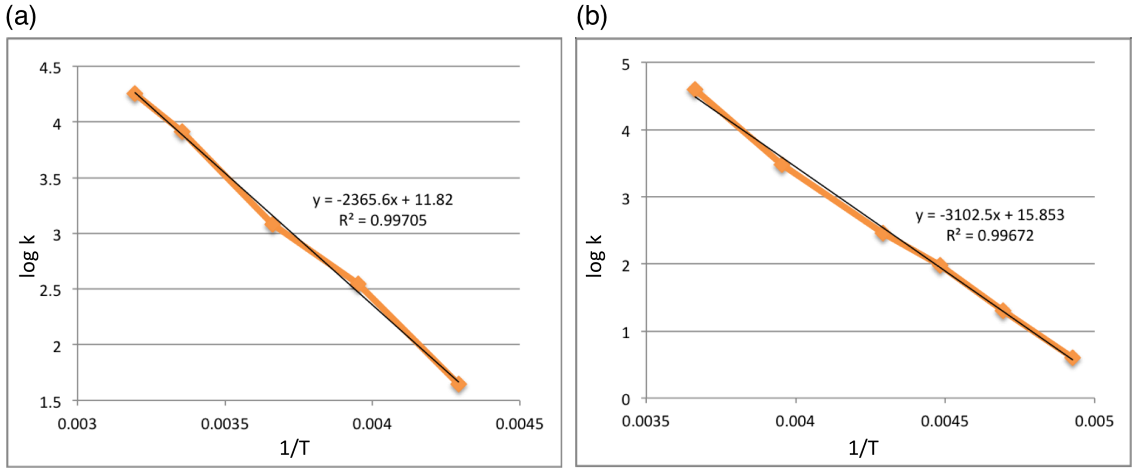

Figure S8. Arrhenius plots for (a) **2a** and (b) **2d**.

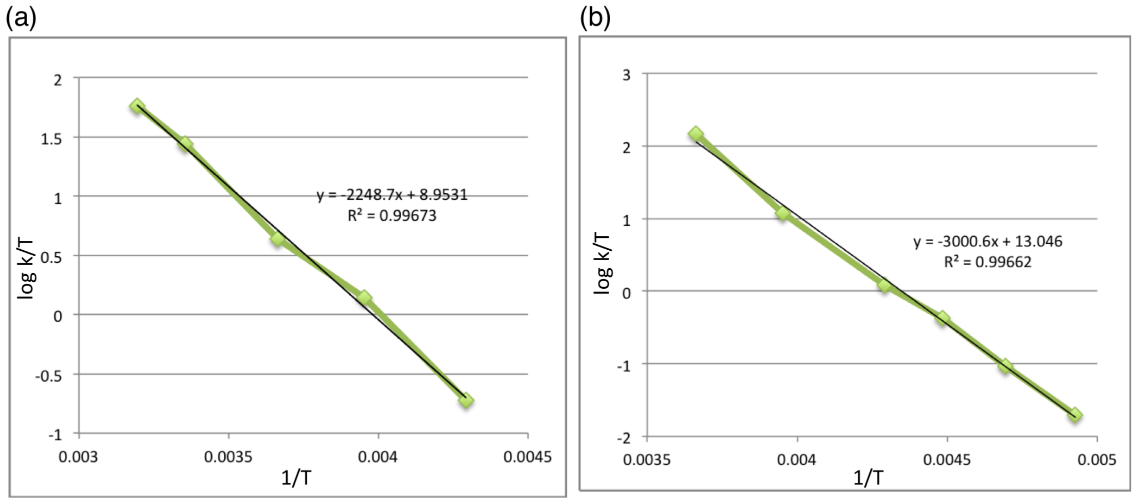

Figure S9. Eyring plots for (a) **2a** and (b) **2d**.

Table S2. Summary of the activation parameters.

	2a	**2d**
E_a [kcal mol^{-1}]	4.69 ± 0.15	6.16 ± 0.18
$\Delta H^{\ddagger}$ [kcal mol^{-1}]	4.46 ± 0.15	5.95 ± 0.17
$\Delta S^{\ddagger}$ [cal mol^{-1} K^{-1}]	–29.38 ± 0.55	–21.26 ± 0.76
$\Delta G^{\ddagger}_{298}$ [kcal mol^{-1}]	13.22 ± 0.31	12.29 ± 0.40

4. Mass Spectra

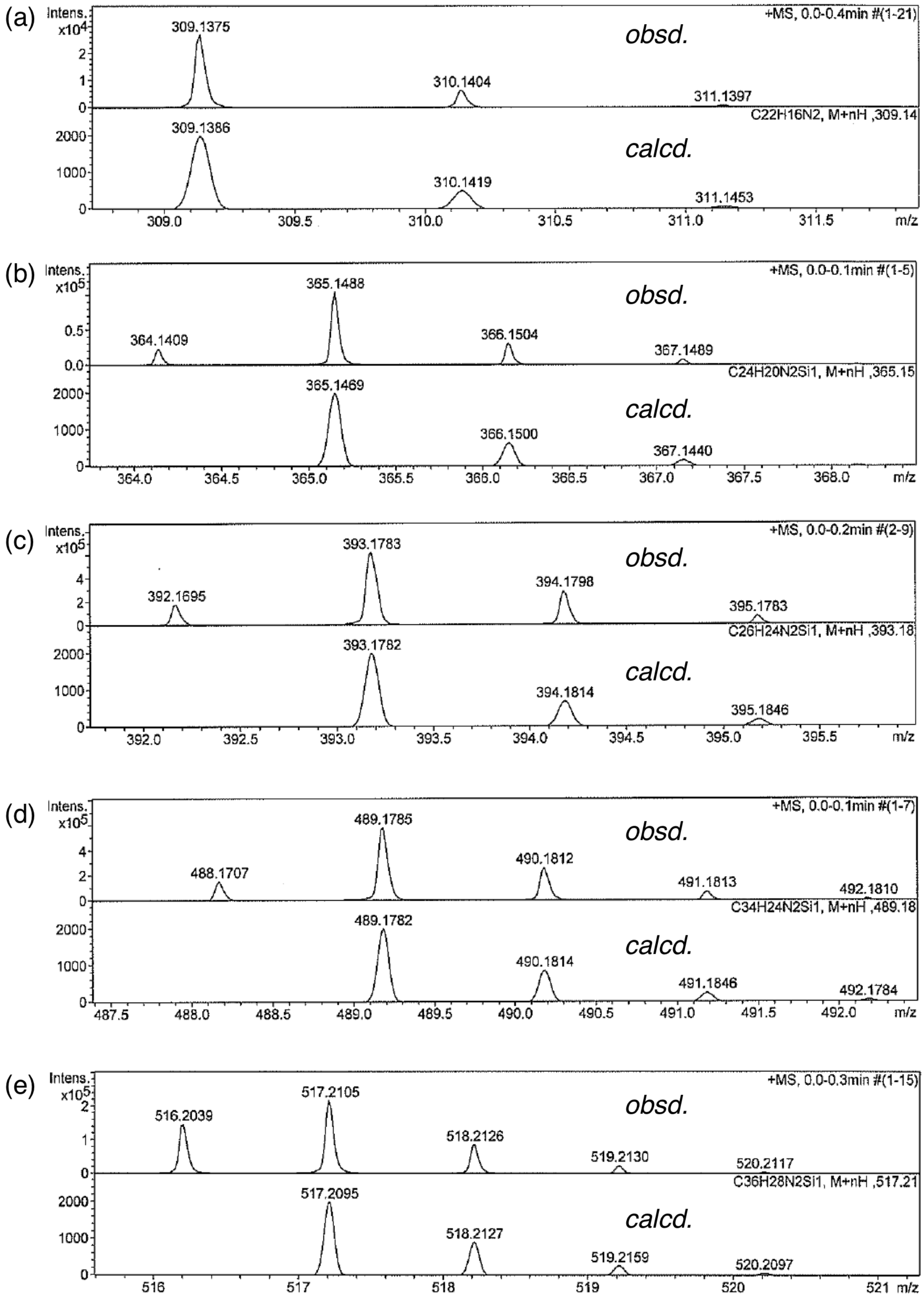

Figure S10. HR-APCI-TOF-MS of (a) **1**, (b) **2a**, (c) **2b**, (d) **2c**, and (e) **2d**. Top: observed, bottom: calculated.

5. X-Ray Crystallographic Details

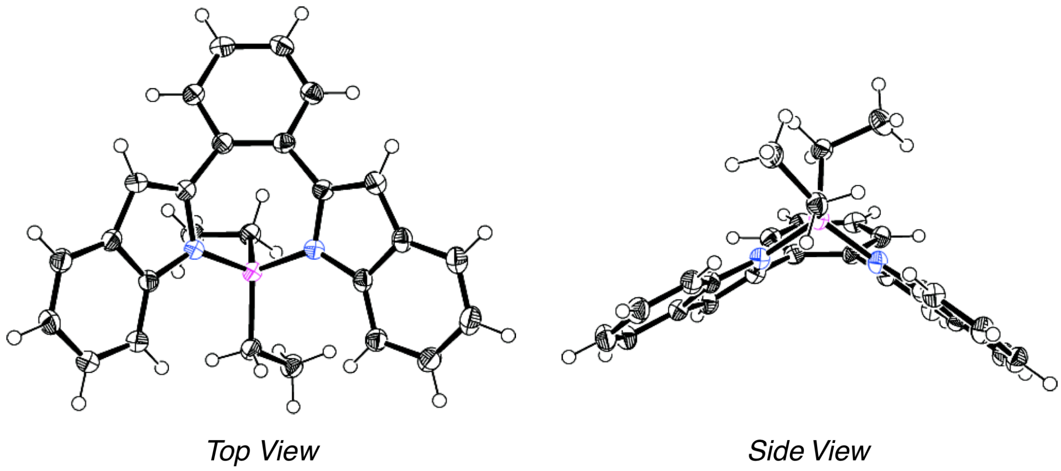

Figure S11. X-ray crystal structure of **2b**. Thermal ellipsoids were scaled to 50% probability.

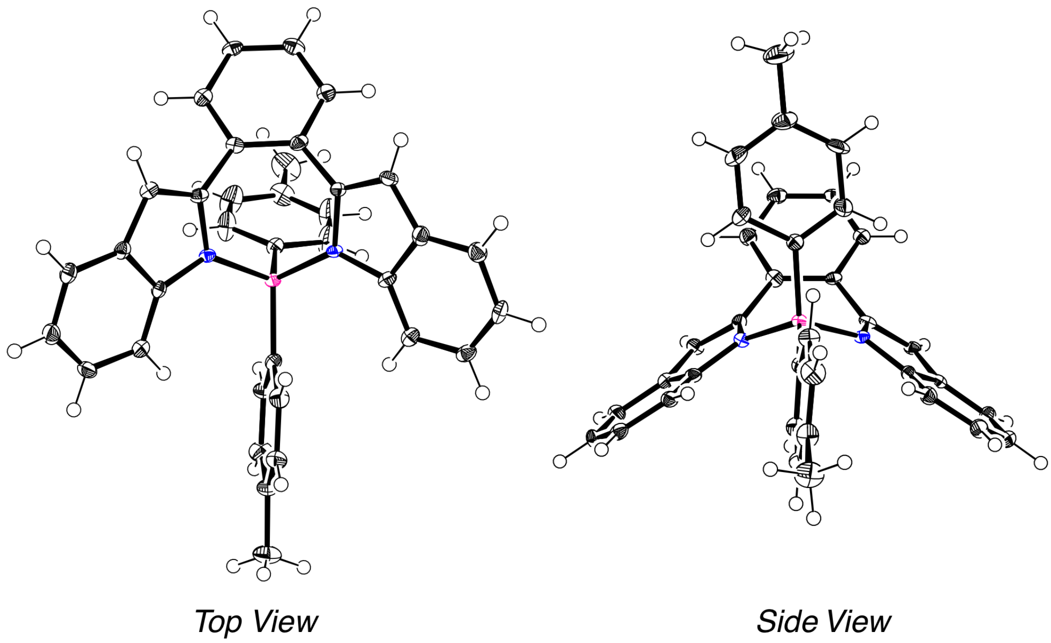

Figure S12. X-ray crystal structure of **2d**. Solvent molecules were omitted for clarity. Thermal ellipsoids were scaled to 50% probability.

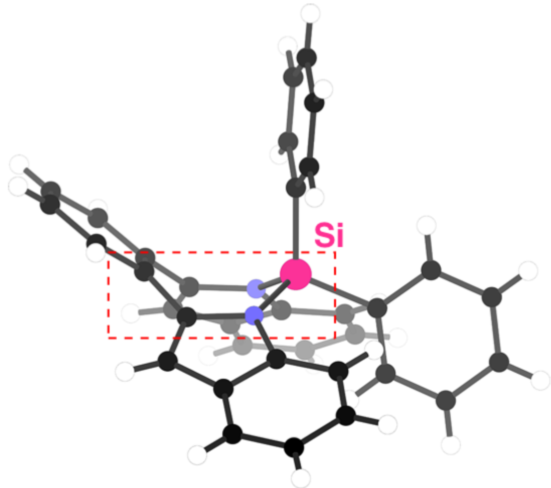

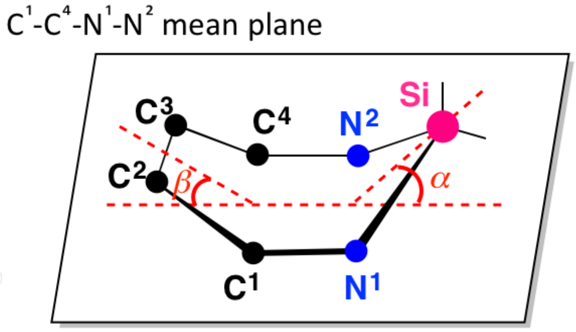

	α[a] (X-ray)	α[a] (DFT)[b]	β[a] (X-ray)	β[a] (DFT)[b]	N–Si bonds (X-ray) [Å]	N–Si bonds (DFT)[b] [Å]
2a	46.11	45.37	42.81	38.31	1.772, 1.765	1.782
2b	47.81	47.40	37.20	37.67	1.763, 1.761	1.786
2c	35.04	36.26	41.37	39.40	1.761, 1.761	1.783
2d	38.82	37.11	38.98	39.49	1.767, 1.761	1.784

[a] The angles α and β are defined as the angles between C^1-C^4-N^1-N^2 mean-plane and N^1-N^2-Si plane, and between C^1-C^4-N^1-N^2 mean-plane and C^1-C^2-C^3-C^4 mean-plane, respectively.
[b] The optimized structures of **2a-d** have been calculated at the B3LYP/6-31G(d,p) level.

Figure S13. Selected bond lengths and structural details of **2a-d** in comparison with those of DFT optimized structures.

* While the α angles in the crystal structures are in consistent with those of calculated ones, the β angles are not in good agreement with calculated values probably due to the crystal packing forces.

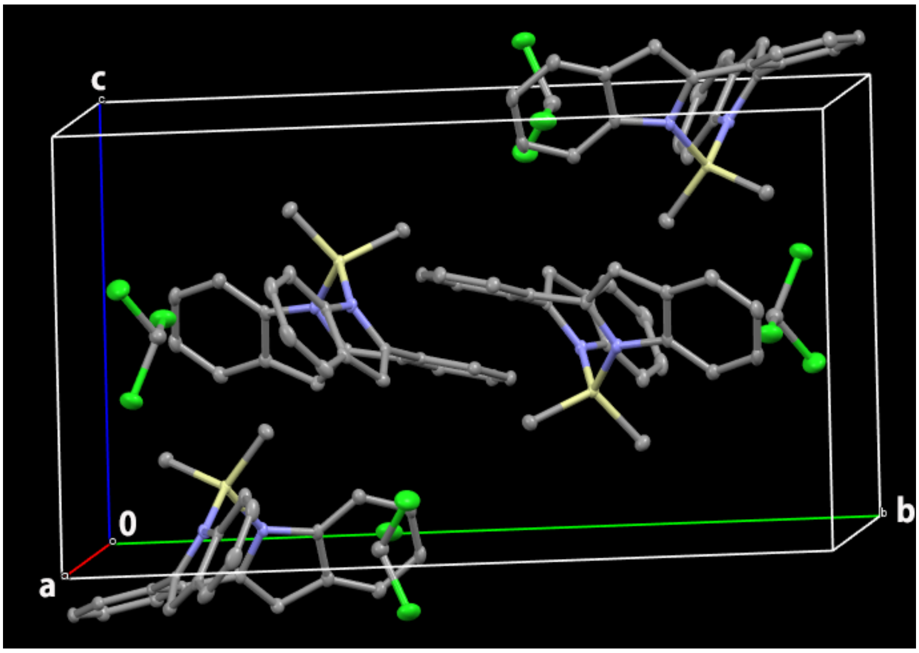

Figure S14. Crystal packing of **2a**. (atom colours, C: gray, N: blue, Si: yellow, Cl: green. Hydrogen atoms are omitted for clarity.)

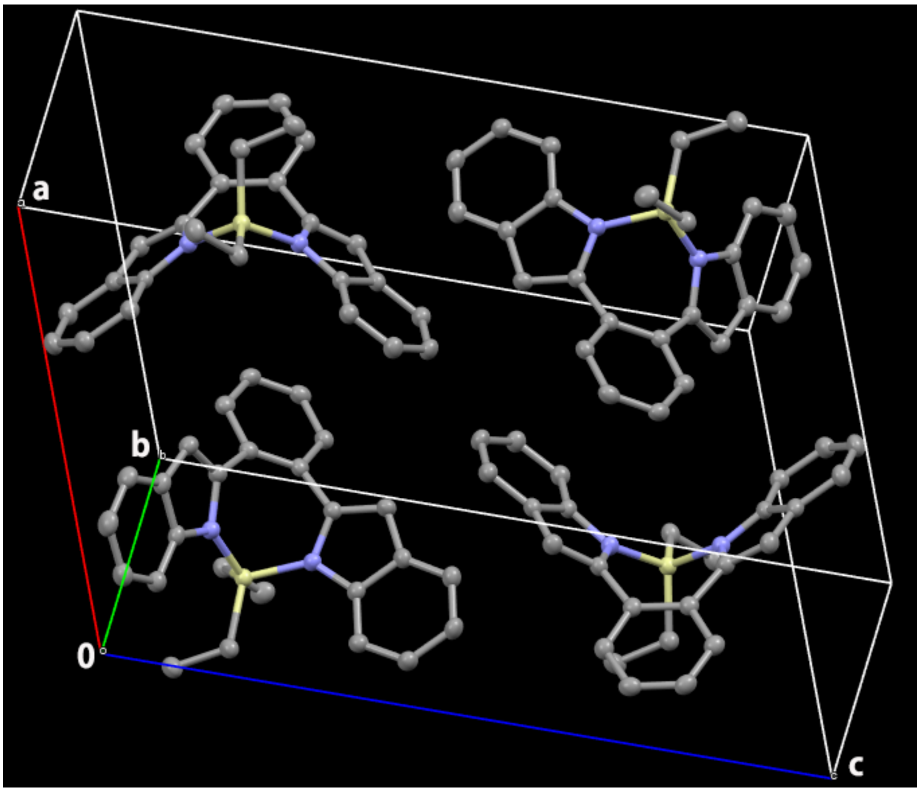

Figure S15. Crystal packing of **2b**. (atom colours, C: gray, N: blue, Si: yellow. Hydrogen atoms are omitted for clarity.)

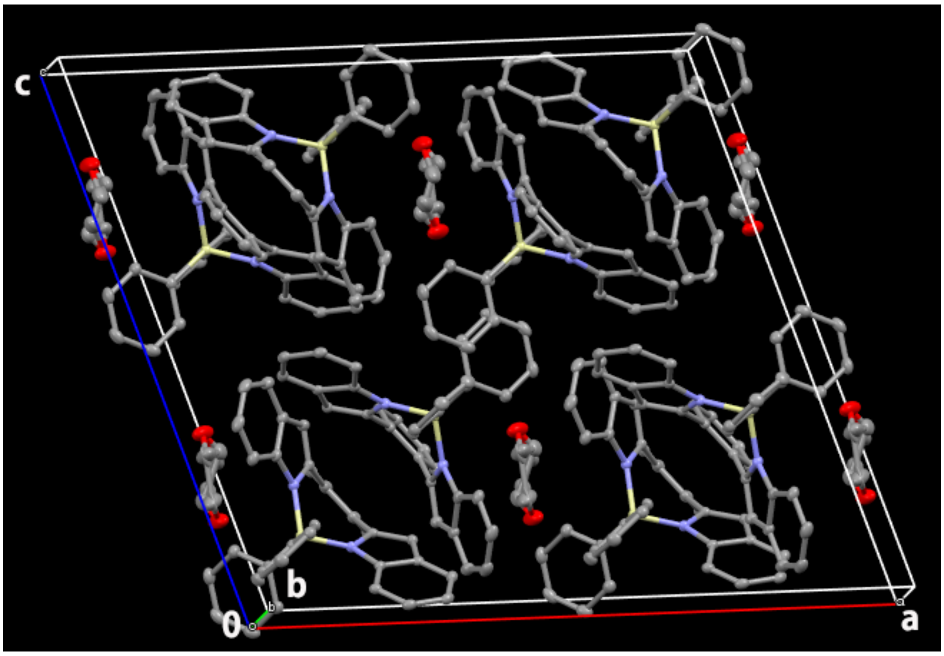

Figure S16. Crystal packing of **2c**. (atom colours, C: gray, N: blue, Si: yellow, O: red. Hydrogen atoms are omitted for clarity.)

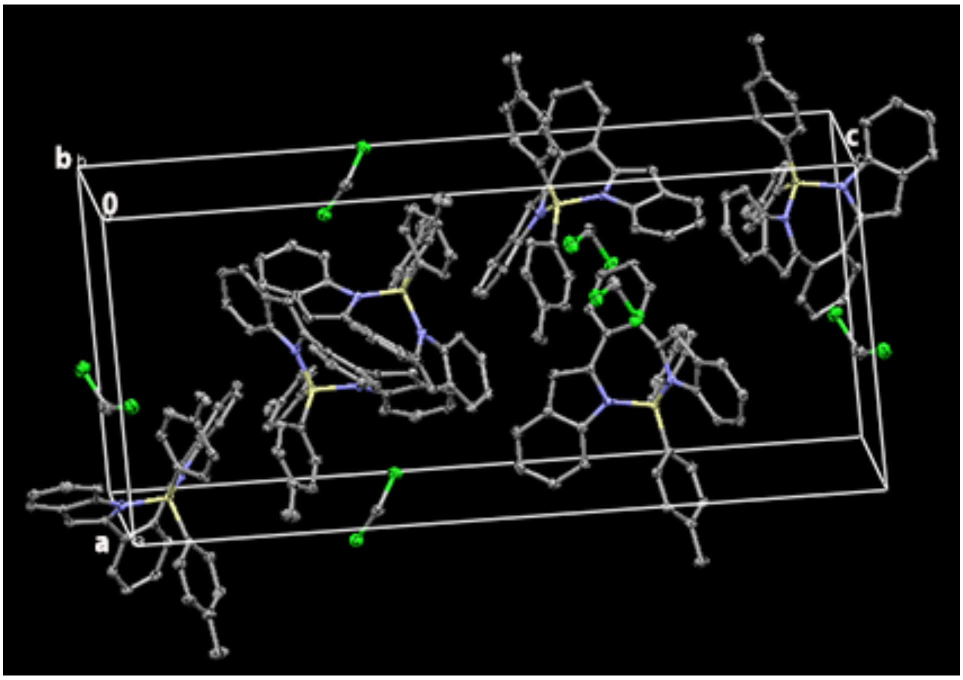

Figure S17. Crystal packing of **2d**. (atom colours, C: gray, N: blue, Si: yellow, Cl: green. Hydrogen atoms are omitted for clarity.)

Table S3. Crystal data and structure refinements for **2a-d**.

Compound	**2a**	**2b**	**2c**	**2d**
Empirical Formula	$C_{24}H_{20}N_2Si_1$ ·($CHCl_3$)	$C_{26}H_{24}N_2Si_1$	2($C_{34}H_{24}N_2Si_1$), ·(C_4H_8O)	2($C_{36}H_{28}N_2Si_1$), (CH_2Cl_2)
M_W	483.88	392.56	1049.39	1118.31
Crystal System	Monoclinic	Monoclinic	Monoclinic	Trigonal
Space Group	$P\ 2_1/c$ (No.14)	$P\ 2_1/a$ (No.14)	$C\ 2/c$ (No.15)	$P\ 3_2\ 21$ (No.154)
a [Å]	10.6810(19)	14.1331(3)	21.767(4)	13.156(3)
b [Å]	19.442(4)	7.81330(10)	12.983(2)	13.156(3)
c [Å]	11.152(2)	18.4958(3)	19.854(4)	28.415(8)
α [deg]	90	90	90	90
β [deg]	101.368(4)	102.1861(10)	108.480(4)	90
γ [deg]	90	90	90	120
Volume [Å^3]	2270.4(7)	1996.68(6)	5321.4(17)	4259.2(18)
Z	4	4	4	3
Density [Mg/m^3]	1.416	1.306	1.011	1.308
Completeness	0.973	0.997	0.985	0.994
Goodness-of-fit	1.039	1.073	1.034	1.030
R_1 [$I > 2\sigma(I)$]	0.0277	0.0461	0.0348	0.0269
wR_2 [$I > 2\sigma(I)$]	0.0751	0.1035	0.0919	0.0275
R_1 (all data)	0.0290	0.0592	0.365	0.0716
wR_2 (all data)	0.0758	0.1126	0.0939	0.0719
Solvent System	$CHCl_3$/ *n*-hexane	THF/heptane	THF/heptane	CH_2Cl_2/MeOH
CCDC	1050753	1050754	1050755	1050756

6. Optical Properties

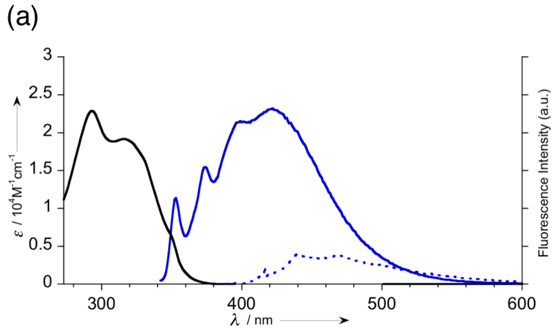

cmpd.	R	$\Phi_{F,DCM}$	$\Phi_{F,powder}$
1	-	0.58	0.09
2a	Me	0.58	0.55
2b	Et	0.58	0.49
2c	Ph	0.65	0.54
2d	Tol	0.62	0.71

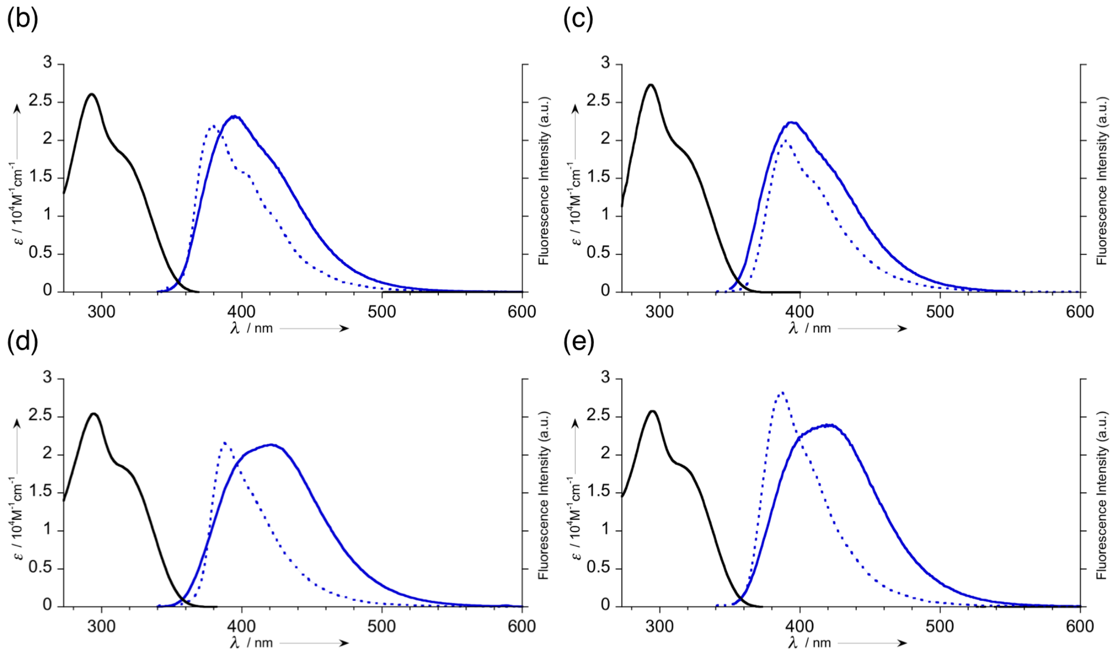

Figure S18. UV/vis absorption and emission spectra of (a) **1**, (b) **2a**, (c) **2b**, (d) **2c**, and (e) **2d** in CH_2Cl_2 (solid lines) and in the solid state (dashed lines).

7. DFT Calculations

All calculations were carried out using the *Gaussian 09* program.[S2] The structures were fully optimized without any symmetry restriction. Calculations were performed by the density functional theory (DFT) method with restricted B3LYP (Becke's three-parameter hybrid exchange functionals and the Lee-Yang-Parr correlation functional)[S3] level, employing a basis sets 6-31G(d,p). Excitation energies and oscillator strengths were calculated with the TD-SCF method at the B3LYP level employing a basis sets 6-31G(d,p).

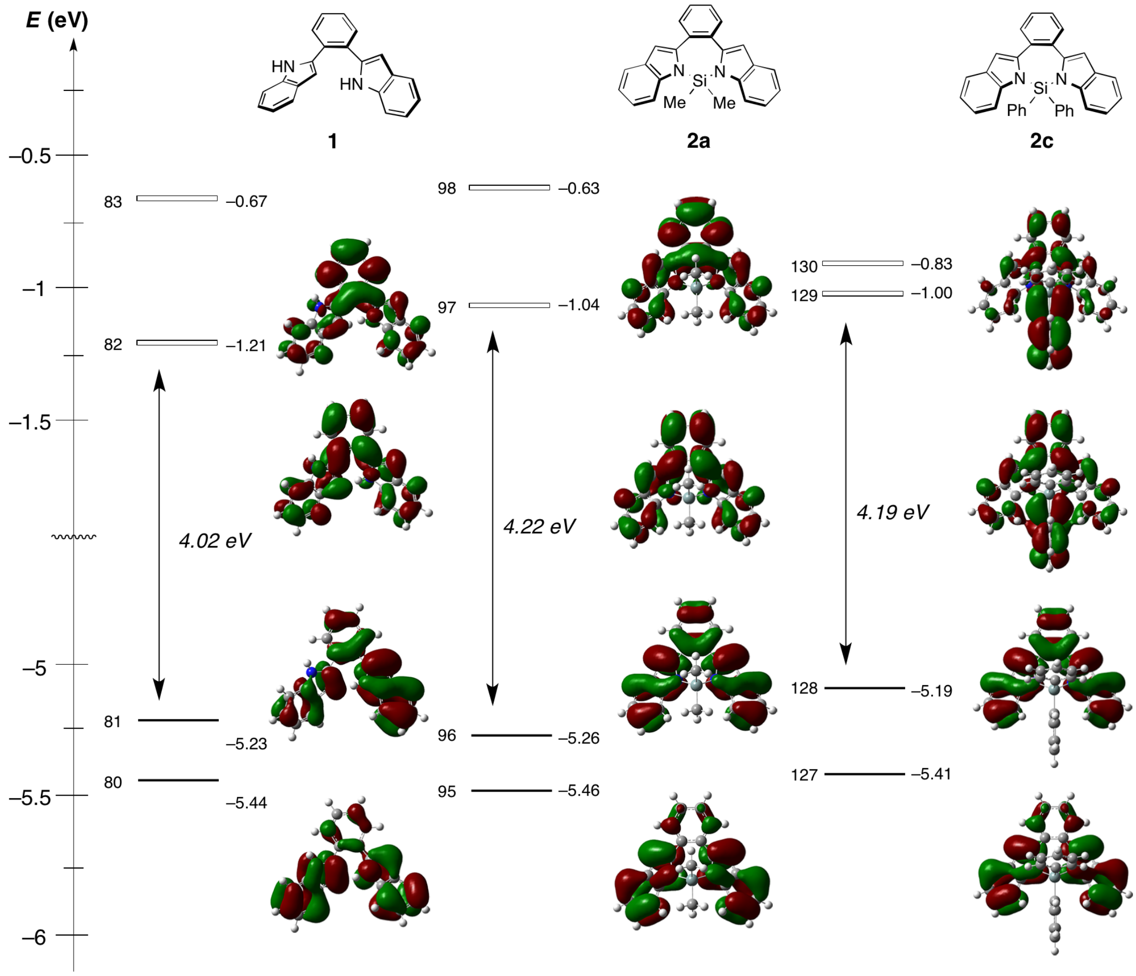

Figure S19. MO diagrams of **1**, **2a** and **2c**.

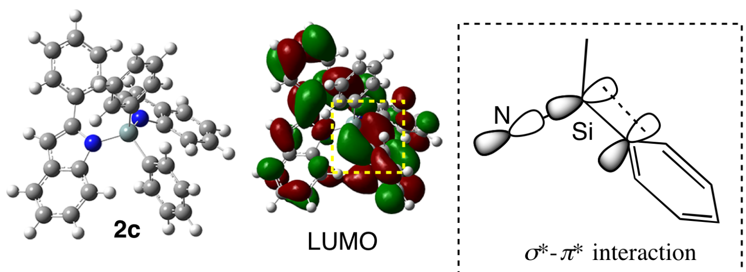

Figure S20. Schematic representation of σ*-π* interaction in the LUMO of **2c**.

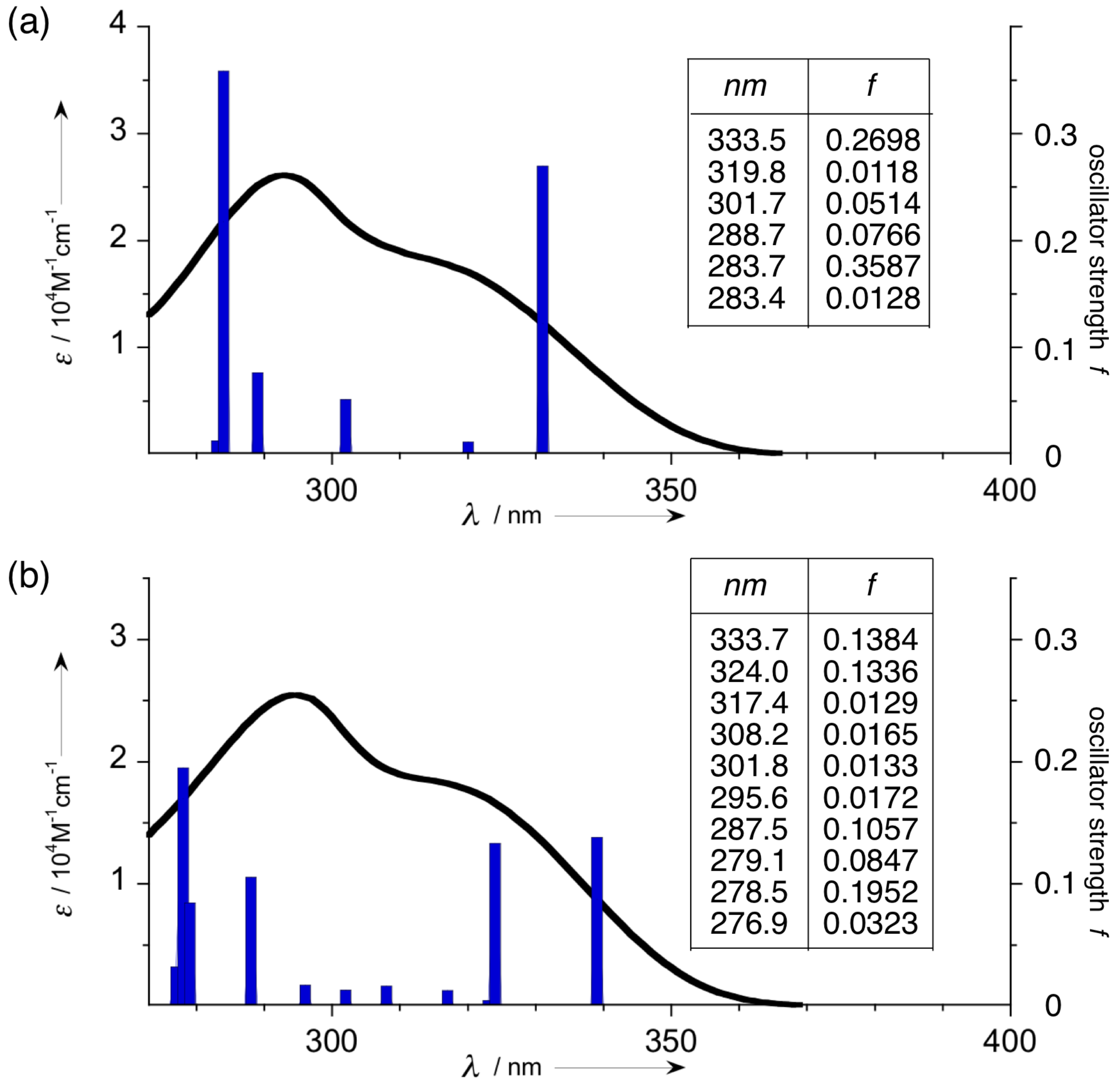

Figure S21. Calculated absorption spectra on the basis of optimized structures (bar) and observed absorption spectra (line) of (a) **2a** and (b) **2c** in CH_2Cl_2.

8. Supporting References

[S1] DNMR3 simulation program: B. W. Tattershall, in DNMRUN and N3PLOT for Windows, Newcastle University, Newcastle, England, 2007; F. P. Gasparro and N. H. Kolodny, J. *Chem. Educ.,* 1977, **54**, 258.

[S2] Gaussian 09, Revision A.02, M. J. Frisch, G. W. Trucks, H. B. Schlegel, G. E. Scuseria, M. A. Robb, J. R. Cheeseman, G. Scalmani, V. Barone, B. Mennucci, G. A. Petersson, H. Nakatsuji, M. Caricato, X. Li, H. P. Hratchian, A. F. Izmaylov, J. Bloino, G. Zheng, J. L. Sonnenberg, M. Hada, M. Ehara, K. Toyota, R. Fukuda, J. Hasegawa, M. Ishida, T. Nakajima, Y. Honda, O. Kitao, H. Nakai, T. Vreven, J. A. Montgomery, Jr., J. E. Peralta, F. Ogliaro, M. Bearpark, J. J. Heyd, E. Brothers, K. N. Kudin, V. N. Staroverov, R. Kobayashi, J. Normand, K. Raghavachari, A. Rendell, J. C. Burant, S. S. Iyengar, J. Tomasi, M. Cossi, N. Rega, J. M. Millam, M. Klene, J. E. Knox, J. B. Cross, V. Bakken, C. Adamo, J. Jaramillo, R. Gomperts, R. E. Stratmann, O. Yazyev, A. J. Austin, R. Cammi, C. Pomelli, J. W. Ochterski, R. L. Martin, K. Morokuma, V. G. Zakrzewski, G. A. Voth, P. Salvador, J. J. Dannenberg, S. Dapprich, A. D. Daniels, O. Farkas, J. B. Foresman, J. V. Ortiz, J. Cioslowski, and D. J. Fox, Gaussian, Inc., Wallingford CT, 2009.

[S3] A. D. Becke, *J. Chem. Phys.,* 1993, **98**, 1372; C. Lee, W. Yang and R. G. Parr *Phys. Rev. B,* 1998, **37**, 785.